

Seafloor roughness estimation employing bathymetric systems: An appraisal of the classification and characterization of high-frequency acoustic data

Bishwajit Chakraborty and K. Haris

Citation: *AIP Conf. Proc.* **1495**, 283 (2012); doi: 10.1063/1.4765921

View online: <http://dx.doi.org/10.1063/1.4765921>

View Table of Contents: <http://proceedings.aip.org/dbt/dbt.jsp?KEY=APCPCS&Volume=1495&Issue=1>

Published by the [American Institute of Physics](#).

Additional information on AIP Conf. Proc.

Journal Homepage: <http://proceedings.aip.org/>

Journal Information: http://proceedings.aip.org/about/about_the_proceedings

Top downloads: http://proceedings.aip.org/dbt/most_downloaded.jsp?KEY=APCPCS

Information for Authors: http://proceedings.aip.org/authors/information_for_authors

ADVERTISEMENT



AIPAdvances

Submit Now

**Explore AIP's new
open-access journal**

- **Article-level metrics
now available**
- **Join the conversation!
Rate & comment on articles**

Seafloor Roughness Estimation Employing Bathymetric Systems: An Appraisal of the Classification and Characterization of High-Frequency Acoustic Data

Bishwajit Chakraborty^a, and K. Haris^a

^a*National Institute of Oceanography (Council of Scientific & Industrial Research), Dona Paula, Goa: 403004, INDIA*

Abstract: The study of the seafloor is important for living and non-living resource estimation along with the related processes identification. To understand the fine-scale seafloor processes, various methods such as application of acoustic remote sensing, seafloor photographic and geological samplings are well established. Among these, the high-frequency single beam echo-sounding system (SBES) and multi-beam echo-sounding system (MBES) became more familiar due to their rapid data acquisition advantages. These systems are extensively used to study the seafloor morphology etc. Seafloor acoustic backscatter information provides fine-scale seafloor roughness and associated sediment processes. The angular and normal incidence backscatter strength data can be utilized to estimate seafloor roughness parameters using physics based numerical inversion models. However, for such applications, the segmentation of the backscatter data is essential, especially before initiating any numerical based models to characterize the seafloor. Under such situations, the employment of the soft-computational techniques e.g., artificial neural networks (ANNs) are found to be suitable for seafloor acoustic data segmentation and classifications. Seafloor studies are carried out at the National Institute of Oceanography, Goa during the last two decades employing similar techniques, and study results related to the seafloor classification and characterizations are documented in this research review.

Keywords: Acoustic remote sensing, multi-beam, single-beam, neural networks, inversion modelling.

PACS: 43.30.Pc, 43.60.Np, 91.50.Ga

INTRODUCTION

Influenced by the land topography and ocean bathymetry, the earth works as an integrated system of interacting bio-geo-physico-chemical processes. The ocean floor acts as an interface between the oceanic lithosphere and hydrosphere, and the interaction (i.e., exchange of mass and energy) zones. Evidence of such interactions on the top seafloor surface morphology is comprehended by the presence of seafloor ripple marks and bioturbation etc. In order to understand the seafloor processes, various methods such as application of acoustic remote sensing, seafloor photographic and geological samplings are well established [1]. The study of the seafloor, employing the above mentioned methods are essential for living and non-living resource estimation and understanding of the related processes. Among these, the high-frequency [2] single beam echo-sounding system (SBES) and multi-beam echo-sounding system (MBES) became more familiar due to their rapid data acquisition advantages, and are mainly used to study the seafloor morphology using bathymetric (measurement and charting of the seafloor) systems [3]. However, apart from acquiring the bathymetric data, echo-sounding systems are also capable to provide

seafloor acoustic backscatter information i.e., idea about the fine-scale seafloor roughness and associated sediment processes (textural aspect) [4]. Backscatter strength acquired using a mapping systems can match with the conventional side scan sonar system and offer side scan sonar data along with the bathymetry [5]. Moreover, the angular backscatter strength data can be utilized to estimate quantitative seafloor roughness parameters: such as sea-water-floor interface as well as sediment volume inhomogeneities using physics based numerical inversion models [6] employing bathymetric systems [7]. However, application of the seafloor segmentation is essential before initiating the applicability of the numerical models to characterize the seafloor. Under such situations, the employment of the soft-computational techniques e.g., artificial neural networks (ANNs) are found to be suitable [8] for seafloor acoustic data segmentation and classifications [9]. Seafloor studies are carried out at National Institute of Oceanography, Goa during the last two decades employing similar techniques. Based on the acquired data, results related to the seafloor classification and subsequent characterizations are presented in this research review.

MEASUREMENTS

Echo-Sounding Data Acquisition

The MBES and SBES are capable of providing both bathymetry and backscatter data. The analysis of bathymetric data provides information regarding depth and reveals seafloor morphological feature. However, the backscatter data contains information about the characteristics of surficial seafloor sediments texture and fine-scale roughness.

MBES Data Acquisition and Processing

During the data acquisition, like other MBES, the Simrad EM 1002 primarily measures the time average of the received backscattered signal envelope in each of its 111 beams. The received signal envelopes are corrected for time variable gain (TVG), predicted beam patterns, and the insonified area. This data then gets recorded in a packet format called “datagram” and are stored along with the other related parameters [10]. However, such recorded data are not directly usable for a correct estimation of the angular dependence backscattering strength. Hence, post processing is essentially to be carried out for the removal of Lambert’s law corrections, actual bottom slope and the insonified area (Fig. 1). If the sonar is not routinely calibrated, the backscatter values obtained after the post processing are probably not accurate (i.e., the reference level is effectively arbitrary), but they are nevertheless likely to be reliable in a relative sense to record differences between sediment types. Consequently, even after the post processing, prior to model-data comparison, there lies a lack of absolute calibration, and a depth-dependent offset (scaling parameter in dB) is required to be added to each of the processed data sets [11]. The real time data acquisition corrections applied by the MBES to the received echo level involves source level, the two-way transmission loss, and the target strength which is included in the local backscattering strength.

Therefore, the insonified area and Lambert's law corrections are needed to normalize the acoustic seafloor image. In normal operational mode, the MBES applies a time varying gain (TVG) to the received signals for compensation of the beam spreading and absorption losses. The purpose of the TVG is to maintain a constant sensitivity for the observation of a given target at any range. The TVG must be predicted before reception (based on previous pings), so that the average signals in the receiver avoids saturation or clipping of the echo envelopes. Here, a comprehensive presentation on the segmentation, classification, and characterization of the processed MBES backscatter data acquired from the central part of the western continental margin of India (WCMI) is being carried out (Fig. 2).

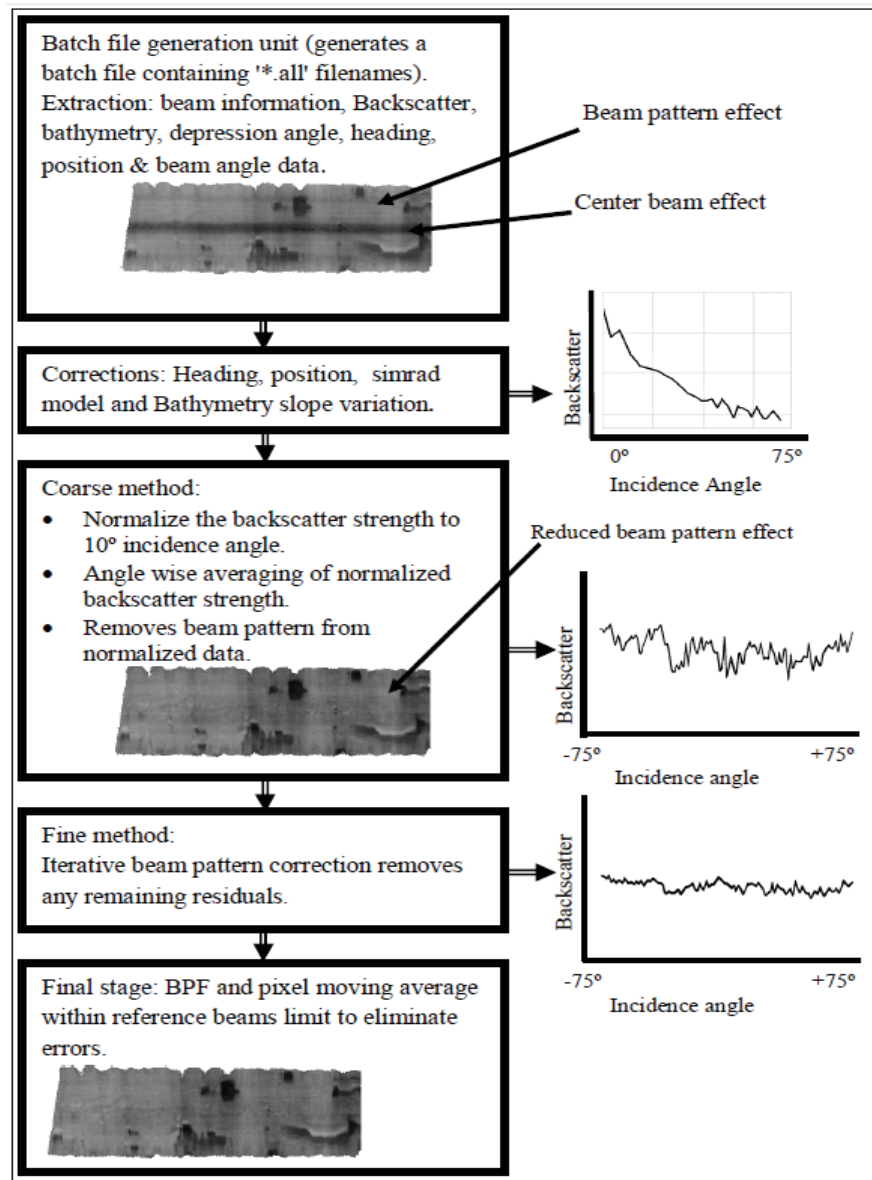


FIGURE 1. Flow chart showing applications of the PROBASI II algorithm for EM 1002 MBES raw backscatter data, reprinted from [10].

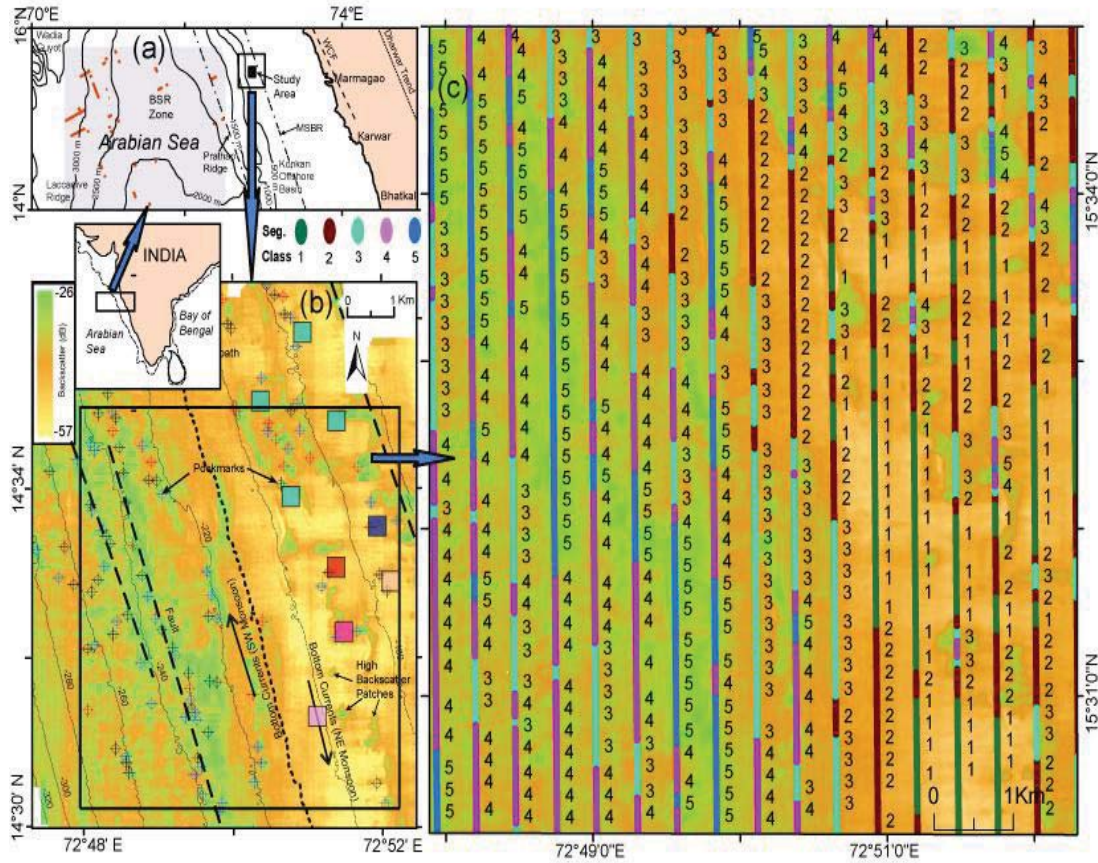


FIGURE 2. Study area showing comprehensive presentation on the segmentation, and classifications of the processed MBES backscatter data tracks acquired from the central part of the WCMI. Five different colours show the segmented section obtained using SOM and FCM.

SBES Data Acquisition and Processing

The present review involves the acquisition of dual-frequency (33 and 210 kHz) backscatter echo data from the central part of the WCMI using a hull-mounted Reson Navitronic NS-420 normal-incidence SBES (the system is customized at the manufacturer's factory to tap echo waveform). The beam widths of the echo sounder transducer for 33 and 210 kHz are 20° and 9°, respectively. The transmission pulse lengths are 0.97 and 0.61 ms, respectively, for 33 and 210 kHz. The SBES outputs were tapped and connected to a PCL 1712L 12-bit A/D converter during the time of data acquisition. The echo data were sampled at 1 MHz, and about 600–800 backscatter pings were acquired along with the sediment samples. In the pre-processing stage, echo data with saturated voltage are removed from the stack. The remaining echo data are subjected to Hilbert transforms to obtain echo envelopes [12]. As we are interested to estimate the values of seafloor sediment properties by optimizing echo envelope matching, the echo envelopes, characterized by a well-defined initial rise and peak amplitude, followed by a slow decay, are selected by visual check for further analysis. Due to the transducer heave motion and small seafloor depth variations over consecutive pings (while recording the data), initial rise

times of the envelopes (which correspond to seafloor depths) are not same for all the echoes collected at a particular location. To obtain stable acoustic signals, echo envelopes are first aligned and then averaged using 20 successive echo envelopes with 50% overlaps (i.e., the echoes are averaged in moving average sense with sequences 1–20, 11–30, and so on till the end of the number of consistent echo envelopes available) (Fig. 3).

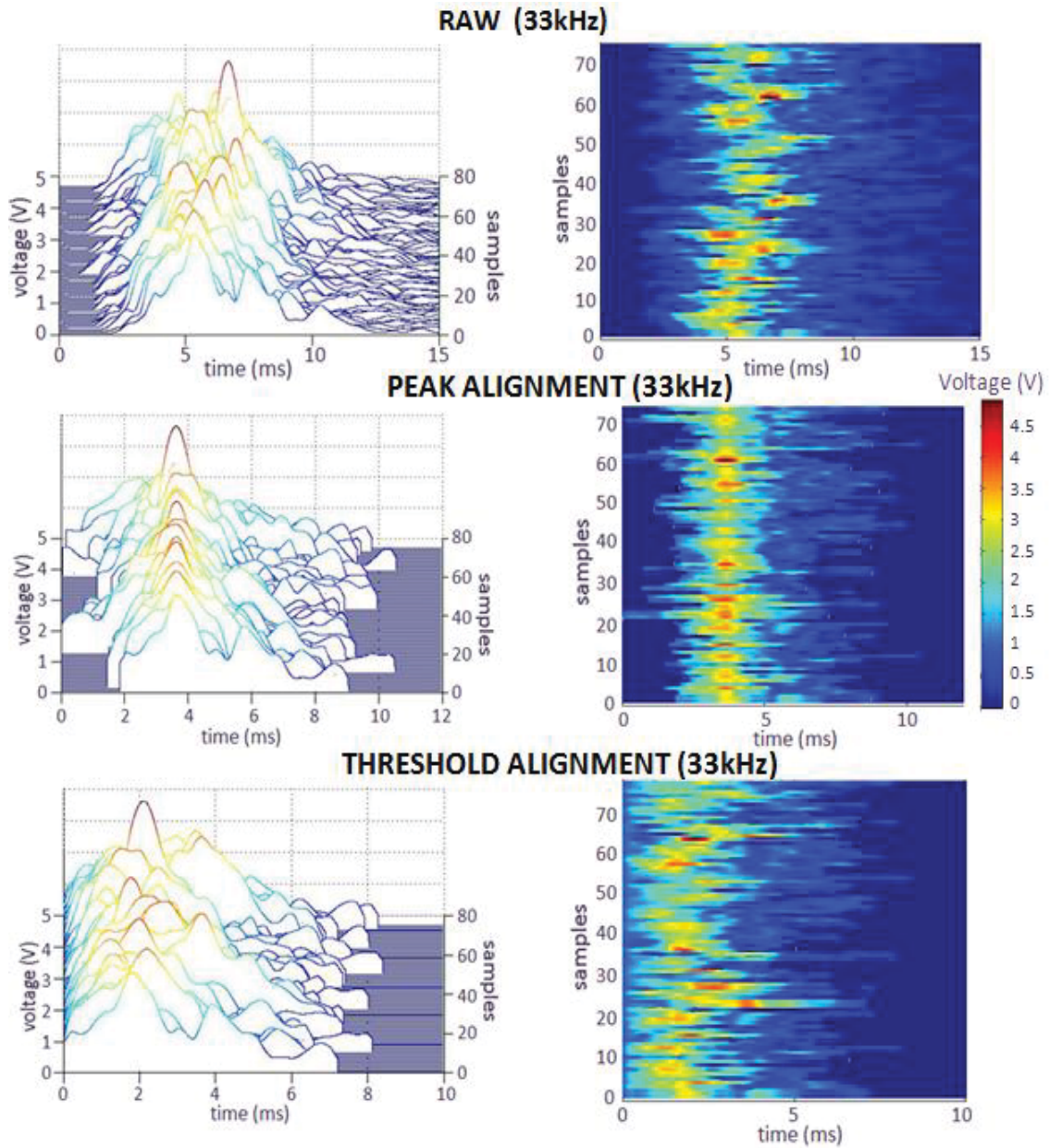


FIGURE 3. Waterfalls and raster plots illustrating the echo-alignment technique for SBES echo-waveform data.

Sediment Ground Truth

Sediment samples were collected using a Van-Veen grab sampler to obtain ground truth on the mean grain size of the sediment. As mentioned earlier, the acoustic backscattering from the seafloor is primarily influenced by the contributions of the energy scattered at the water–sediment interface and from the sediment volume. Interface scattering can be described by the interface roughness coupled with acoustic impedance [13]. Volume scattering depends on the water-sediment interface characteristics for transmission of the energies and then absorption inside the sediment volume. A significant contribution, due to volume scattering (in addition to interface scattering) from various scatterers (e.g., shells, pebbles, gas bubbles, living organisms, sediment layering etc.), is expected at 33 kHz due to greater penetration of energies. However, the effect of volume scattering is expected to decrease (in contrast with the interface scattering) with the increase in the acoustic frequency because of enhanced absorption. The absorption in seafloor sediments typically varies in the range 0.1-1.0 dB/wavelength. Here, the acoustic wavelengths for 33 to 210 kHz vary from 4.5 to 0.7 cm, respectively. Thus, surficial sediments collected by a grab sampler can be considered as the representative of sediment probed by the echo sounder to estimate providing quantitative information on seafloor sediment. The percentage compositions of sand, silt, and clay in surface sediment samples are determined in the laboratory using a laser particle size analyzer. Shepard's scheme is used to decide the sediment types based on the percentage compositions of sand, silt, and clay. The analyses reveal four types of sediments where SBES data were acquired. They are: clayey silt, silt, silty sand, and sand. The sorting coefficients for clayey silt and silt samples vary within a range of 1.32ϕ to 1.96ϕ , whereas for silty sand and sand samples the sorting coefficients vary within 0.99ϕ to 2.24ϕ .

TECHNIQUES EMPLOYED AND RESULTS

MBES Data Segmentation Using Artificial Neural Networks

The non-stationarity of the seafloor depth and image information is obviously a major obstacle to any statistical analysis since most statistical procedures presume that the input is stationary. It is therefore important to attempt segmentation of the non-stationary data into stationary intervals. Hence, it is necessary first to divide the data set into stationary one [14], and then estimate the statistical characteristics of each segment separately. In the present context, typical stages of seafloor studies include segmentation, classification and characterization in terms of estimating the roughness etc. Once the seafloor backscatter image / topography are segmented then they undergo classification and subsequent characterization for geo-acoustical parameter estimation. The objective of seafloor sediment classifications studies using remote acoustic methods mainly depends on two important parameters: the number of sediment classes prevailing in the area [15], and the selection of the features having prominent discriminating characteristics [8]. Soft computational techniques such as: Artificial Neural Networks (ANNs) were employed for seafloor acoustic data

segmentation and subsequent classification [8], [16] for MB acoustic backscatter data. For online application, the ANN-based seafloor classifier serves as a real time classifier into different known classes. ANN architecture, viz. Kohonen's Self-Organizing Map (SOM) has been employed for seafloor segmentation and for accurate classification using LVQ network for MB backscatter data. Similar attempt was also employed to echo-waveform data from western continental shelf [17]. Also, seafloor data segmentation and classifications using unsupervised architecture called Kohonen's self-organizing map (SOM) and fuzzy C-means (FCM) algorithm using echo features extracted from backscatter returns are recorded for SBES at 33- and 210-kHz frequencies [14]. The classical uses of SOM are well documented (references are provided here) for SBES echo-waveform, and MBES backscatter data to obtain the idea about the number of classes present in a data set based on the inherent discrimination ability of the feature vectors. The approximate number of classes obtained from SOM analysis may vary based on the input vector chosen for unsupervised training, which may influence the subsequent analysis with supervised fine-tuning. Therefore, a SOM-based method is used to estimate the possible maximum number of prevailing seafloor classes.

Here, SOM is applied to MBES backscatter data, and the structure of the Kohonen's algorithm is discussed [18]. The learning algorithm organises the nodes in the grid into local neighbourhoods that act as feature classifiers on the input data. The topographic map is autonomously organised by a cyclic process of comparing input pattern to vectors "stored" at each node. Where inputs match the node vectors, that area of the map is selectively optimised to represent an average of the training data for that class. From a randomly organised set of nodes the grid settles into a feature map that has local representation and is self-organised. The algorithm details are given below:

1. *Initialise network:* - Define $w_{ij}(t)$ ($0 \leq i \leq n-1$) to be the weight from input i to node j at time t . Initialise weights from the 'n' inputs to the nodes to small random values. Set the initial radius of neighbourhood around node j , $N_j(0)$, to be large.
2. *Presenting input:* - For one iteration t , one features vector $X = [x_0(t) \ x_1(t) \ \dots \ x_{n-1}(t)]$ where $x_i(t)$ is the input to node i , is presented to the matrix.
3. *Calculating distances:* - Compute the distance ' d_j ' between the input and each output node j , and is given by $d_j = \sum [x_i(t) - w_{ij}(t)]^2$.
4. *Selecting the minimum distance:* - The output neuron that minimises ' d_j ' is designated to be the firing neuron, noted j^* .
5. *Updating weights:* - The weights are updated for neuron ' j^* ' and its pre-defined neighbours. The size of the neuron firing neighbourhood must decrease as the number of iterations increases. New weights are: $w_{ij}(t+1) = w_{ij}(t) + \eta(t)(x_i(t) - w_{ij}(t))$ where $\eta(t)$ is the learning function that decreases in time and such that: $0 < \eta(t) < 1$.
6. Repeating by going to 2.

SOM application was performed on the backscatter data acquired off Goa coast along the WCMI at depth ranging from 145 m in the northeast to 330 m in the southwest. Backscatter imagery was acquired using Simrad EM 1002 MBES operating at frequency of 95 kHz. The survey covers an area of nearly 105 km² and reveals 112 pockmarks. During the previous study, the backscatter data have been used to

understand the morphology of pockmarks from the western continental margin of India [19]. These pockmarks are caused by the presence of gas or fluid seepages escaping from the subsurface along the fault. As a continuation, the statistical characterisation of seafloor [20] and the fractal analyses of backscatter image blocks allowed to understand the processes acted in this region. MBES backscatter data of all 17 tracks (each track consisting of 466 data points) was segmented into five classes signifying five seafloor types (Fig. 2).

Kohonen's self-organising map (SOM) was used to infer maximum possible number of classes. The two feature vectors using the pixel data such as i) backscatter strength and ii) seafloor roughness using corresponding bathymetry from the study area was applied as input vectors. In order to know the number of classes, SOM was applied once to the whole data. At each iteration ' t ' of this given training-testing process, a features vector were presented to the random weight matrix and the closest neuron was selected to be the firing neuron, and these neurons were updated using the learning function $0.4/t^{0.2}$. As ' t ' increases, the neighbourhood was reduced to one, i.e., at the end, only the firing neuron was updated. Training stops when the error is less than 10^{-30} or at the 2000th iteration [14]. The output neuron number was chosen as 50 based on the several trials. The excited neurons obtained during every testing process are plotted with respect to the neuron positions in a bar diagram. If the testing shows that the winning neuron exists within the range of the trained neuron position, then it is assumed as belonging to the same class, where the data were trained earlier. Otherwise it is considered as a new class. The maximum number of classes is estimated by counting the presence of the number of prominent fired neurons (bars). At the end of each process, the percentages of times the different neurons have been excited, i.e., firing, was plotted in a bar diagram, with respect to the neuron number. The maximum number of classes is equal to the number of occurrences of surrounding 20% of the highest firing of neurons. The 20% criterion has been chosen from a few trial runs [Fig. 4(a)].

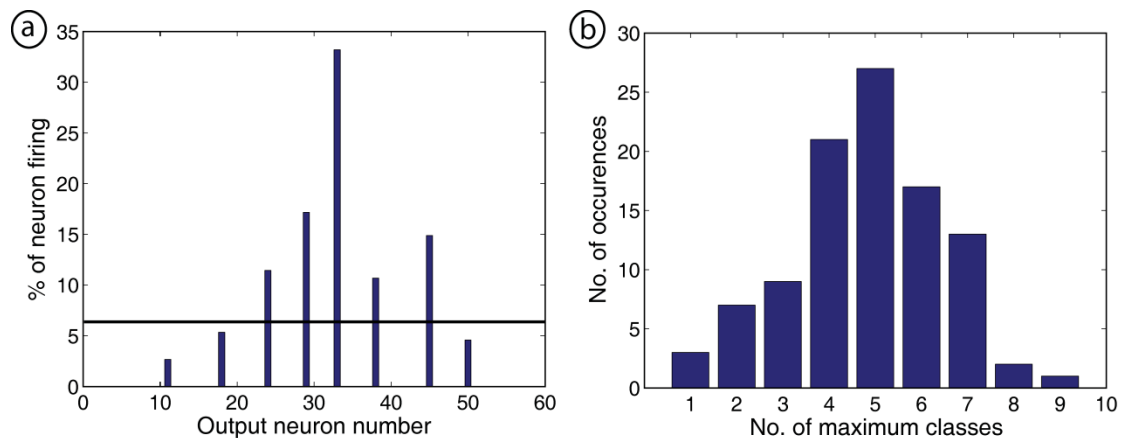


FIGURE 4. (a) The horizontal black line represents the line of 20% of the maximum number of firings, and 5 bars above the line indicating 5 classes obtained from the training-testing process. (b) Histogram of the number of occurrences of maximum number of classes obtained from the 100 training-testing process of SOM analysis.

The training-testing process was repeated for sufficient times (100). For each training-testing process, the number of classes found was determined from the numbers of occurrences versus the numbers of classes are plotted in a histogram. The number of classes occurred maximum number of times is considered to be the number of classes available in the data [Fig. 4(b)]. This process provides the number of classes available in a given data set without any prior information [16]. Once, no. of classes present in the data set is known then the next step is to identify the classes within the data. So, fuzzy clustering method (FCM) [14] was applied to the track data, which results in five segments within the 17 chosen tracks. The statistical application of the firing neuron of SOM output and subsequent use of FCM provides segmented backscatter dataset having five classes (Fig 5).

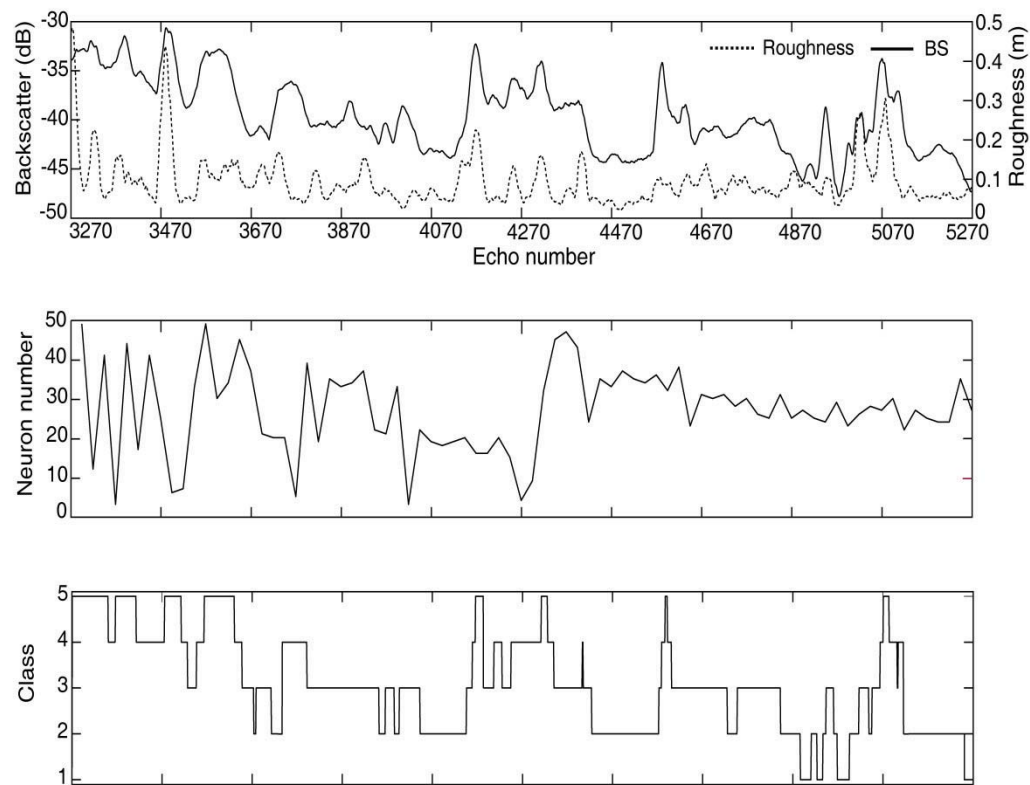


FIGURE 5. (a) Plot of the input feature vectors (backscatter and roughness), (b) Neurons firing corresponding to the input vectors fed into SOM, and (c) Classification of the data points done using FCM, for tracks 7-11.

Numerical Modelling to Estimate Seafloor Roughness Parameters

In this section, we compare the estimated seafloor parameters of the angular backscatter MBES data with the echo envelope data of normal incidence SBES using the composite roughness scattering model for the study locations on the continental shelf [Fig. 6(a)] [11]. Figure 6(b) provides raw and processed MBES data from the

locations. This study provides a comparison between the estimated seafloor parameters at three frequencies to assess the model performance. The results obtained using three frequencies echo sounding data are analyzed and compared to the ground truth data. Figure 6(c) shows representative model-data fit for a geologically distinct sediment province. For simplicity, silty-sand and sand sediments are referred as coarse sediments (with estimated $M_\varphi < 4\varphi$); and clayey-silt and silt sediments are fine sediments (with estimated $M_\varphi > 4\varphi$).

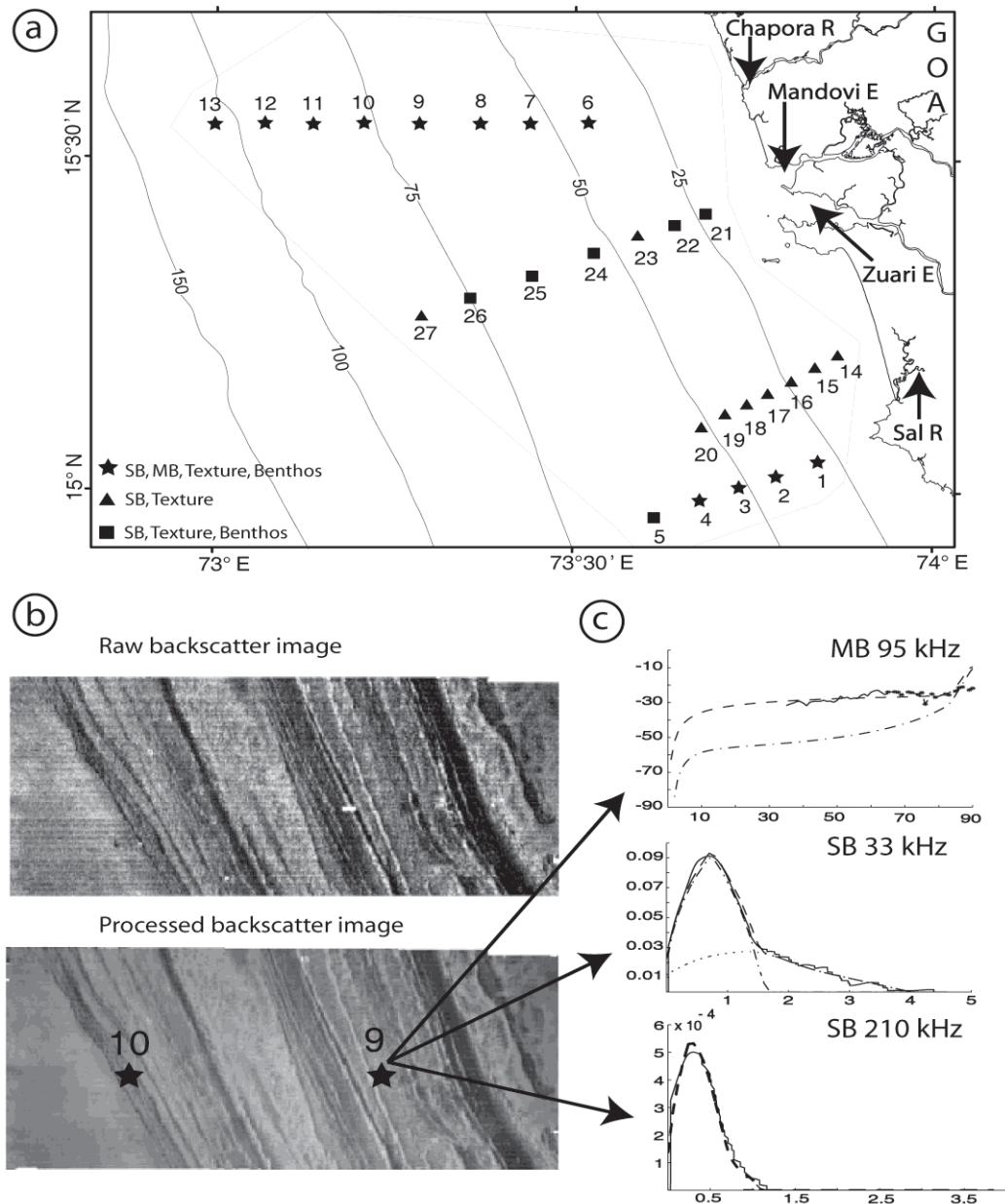


FIGURE 6. (a) Shows the study area with type of data collected from the shelf seafloor. The depth contours are in meters. The acoustic data was sampled with EM 1002 MBES and RESON-NS 420 SBES. (b) Show typical application of the PROBASI II algorithm for EM 1002 backscatter data. Presented in (c) is the examples of inversion model data output, reprinted from [11].

Estimated Mean Grain Size (M_ϕ) Parameter

The peak amplitudes of echo envelopes primarily depend on the impedance contrast between the water and seafloor sediments. In surficial sediments, the impedance contrast is often correlated with the mean grain size of sediments. The estimated mean values of M_ϕ of surficial sediments obtained with echo envelope inversions from the study locations are found to correlate well with the measurements (95% of confidence limit). The estimated values of M_ϕ obtained from the inversions of angular backscatter strength of MBES also should correlate with the measurements (based on sediment ground truth) and / or information from [12]. In view of this, the estimated M_ϕ values for three different acoustic frequencies are presented as a function of the measured M_ϕ values [Fig. 7(a)]. On the whole, the estimated M_ϕ values agree well with the measured sediment data, having correlation coefficients of 0.97, 0.98, and 0.96 for 33, 95, and 210 kHz, respectively.

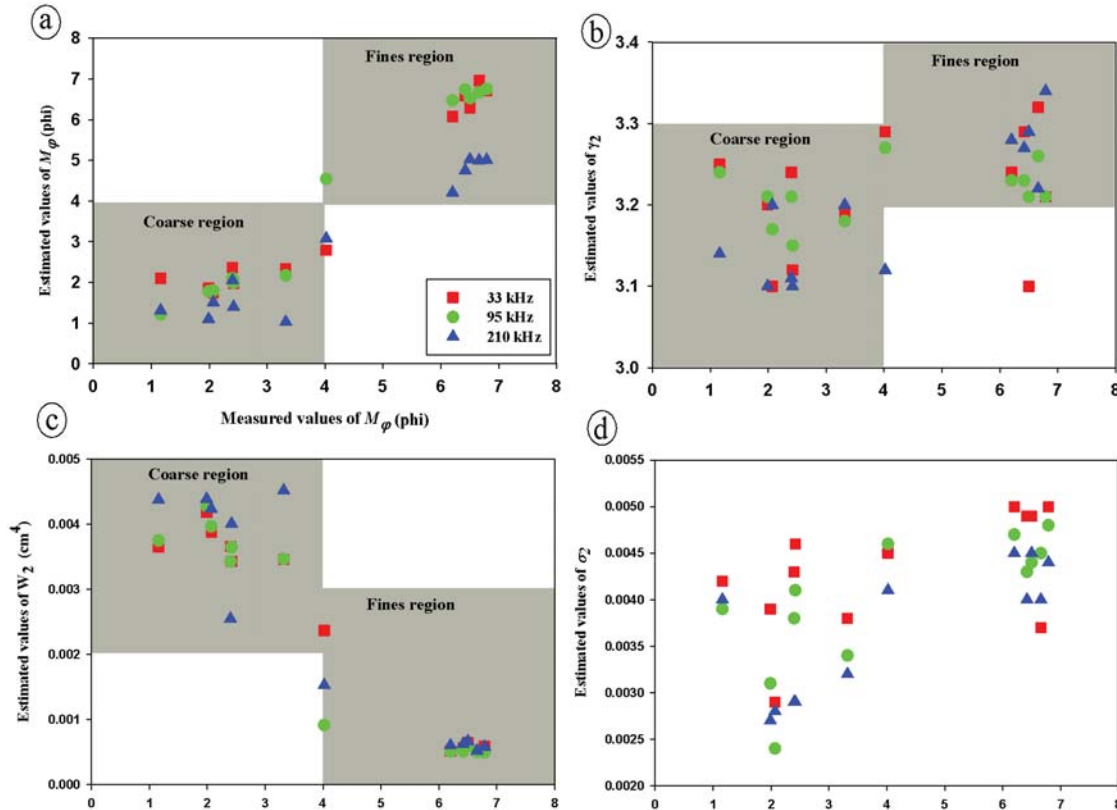


FIGURE 7. The scatter plot showing the relationship between the measured values of M_ϕ (phi) with (a) The estimated values of M_ϕ (phi), (b) The estimated spectral exponent γ_2 , (c) The estimated spectral strength parameter w_2 (cm⁴), and (d) The estimated sediment volume parameter σ_2 for the three inversion cases. The two blocks in the figures represents the boundaries of estimated parameters for coarse and fine sediments, reprinted from [11].

Estimated Seafloor Roughness Parameters (γ_2 and w_2)

An analysis is carried out using the estimated seafloor roughness parameters of MBES and dual-frequency SBES data [Fig. 7(b)]. For coarse sediments, the overall average estimates of γ_2 are found to be 3.18 ± 0.061 , 3.19 ± 0.032 , and 3.14 ± 0.047 , respectively, for 33, 95, and 210 kHz [11]. But for fine sediments, the overall average estimates of γ_2 are 3.23 ± 0.085 , 3.22 ± 0.020 , and 3.28 ± 0.043 , respectively, for 33, 95, and 210 kHz. It is observed that higher values of γ_2 are associated with fine sediments, and in contrast lower values of γ_2 are associated with coarse sediments. The seafloor roughness power spectrum estimated from the relative height measurements is a characterization of the variance of the size and periodicity of the seafloor height fluctuations as a function of the spatial frequency. The roughness power spectrum is often parameterized using a power law by the slope and intercept of the linear regression line through the points of the periodogram estimate in *log-log* space. The parameters γ_2 and w_2 used in the scattering model of [6] are actually the slope and intercept, respectively, of the 2D roughness power spectrum. A wide range of these 2D roughness power spectrum parameters indicate that the majority of the values of the 2D spectral exponent are confined within the limits of 2.90 to 3.30 for coarse sediments and 3.20 to 3.50 for fine sediments [11]. In the present study the estimated γ_2 values are found to be in agreement with the published data, but have a narrower range of values. Several field experiments revealed [21], [22] that the majority of the measured values of 2D spectral strength (w_2) are greater than 0.002 cm^4 for coarse sediments, and are restricted to values around 0.003 cm^4 for fine sediments. The scatter diagram between the measured values of M_ϕ and estimated w_2 [Fig. 7(c)] revealed that the values of w_2 are less than 0.001 cm^4 for fine sediments and are confined within 0.002 to 0.005 cm^4 for coarse sediments from all the three inversion results. Moreover, for coarse sediments, the overall average estimates of w_2 are found to be 0.0037 ± 0.00028 , 0.0037 ± 0.00032 and 0.0040 ± 0.00074 , respectively, for 33, 95, and 210 kHz. But for fine sediments, the overall average estimates of w_2 are 0.00057 ± 0.000052 , 0.00052 ± 0.000043 , and 0.00060 ± 0.000054 , respectively, for 33, 95, and 210 kHz. On the whole, the values of w_2 at the three frequencies are found to be in good agreement with the published information. It is observed that the estimated values of w_2 are well clustered, having less fluctuations for fine sediments than for coarse sediments at all acoustic frequencies. Moreover, it is also observed that higher values of w_2 and lower values of γ_2 are associated with coarse sediments, while lower values of w_2 and higher values of γ_2 characteristics are found for fine sediments.

Estimated Sediment Volume Parameter (σ_2)

The sediment volume parameter (σ_2) controls the level of the tail portion of the echo envelope. Generally, σ_2 values are functions of the seafloor sediment type (fine or coarse) and seafloor inhomogeneities. Jackson and Briggs [23] demonstrated dominant sediment volume backscatter for finer sediment, and Jackson *et al.*, [6] considered it as a free parameter with a maximum value up to 0.004 for soft sediment. However, Stewart and Chotiros [24] have experimentally shown that the limit imposed

for soft sediment is low, and the sediment volume scattering coefficient is usually much higher than the predicted value. Nevertheless, it is preferable to use the estimated σ_2 as a fitting parameter for different locations as a means to understand the seafloor processes. The sensitivity analysis of σ_2 on the echo envelope shape indicates that as σ_2 increases the contribution of sub-bottom scattering becomes prominent near the tail portion of the echo envelope. The peak amplitude of the total echo envelope, however, changes marginally with an increase in the value of σ_2 . For coarse sediments, the overall average estimates of σ_2 are found to be 0.0039 ± 0.00059 , 0.0034 ± 0.00063 , and 0.0031 ± 0.00048 , respectively, for 33, 95, and 210 kHz. But for fine sediments, the overall average estimates of σ_2 are 0.0047 ± 0.00056 , 0.0045 ± 0.00021 , and 0.0043 ± 0.00026 , respectively, for 33, 95, and 210 kHz. These values of σ_2 are necessary to provide reasonable model-data fits at the three acoustic frequencies [Fig. 7(d)]. Jackson and Briggs [23] reported that the volume scattering will be dominant for soft sediments. The experiment conducted by them revealed that the predicted model matches well with the observed data, if relatively high values of σ_2 (0.004 to 0.006) are used for soft sediments. Thus, large values of σ_2 may be required to get the best model-data fit for soft sediments [11].

ACKNOWLEDGMENTS

We acknowledge permission from the Director, NIO to publish this work. One of the author (BC) is grateful to the organizers of the 3rd *International conference of Ocean Acoustics*, especially to Dr. Jixon Zhou (Georgia Institute of Technology) and Dr. Jeffrey Simmen, (Director, APL, University of Washington) for invitation to deliver the “regular invited talk”. Travel support from the Office of the Naval Research Global (ONRG), USA to BC is also gratefully acknowledged. We are also indebted to Dr. Robert Bolia, Associate Director, ONRG, for his help in many ways, and to Dr. Kevin Williams, APL, University of Washington, for extensive discussions regarding this research. KH acknowledges support from the Council of Scientific Research, New Delhi for their fellowship scheme to carry out the research. Finally, we express our gratitude to Andrew Menezes, William Fernandes, and Dr. Baban Ingole of NIO for their support.

REFERENCES

1. E. Seibold and W. H. Berger, *The Sea Floor: An Introduction to Marine Geology* (Springer-Verlag, Berlin, 1993).
2. D. R. Jackson and M. D. Richardson, *High-Frequency Seafloor Acoustics* (Springer-Verlag, New York, 2007), Chap. 13, pp. 331-376.
3. B. Chakraborty and W. Fernandes, "Bathymetric techniques and Indian ocean application," in *Bathymetry and its application*, edited by P. Blondel, Croatia: InTech, 2012, pp. 3-30 (www.intechopen.com).
4. C. de Moustier, "Beyond bathymetry: mapping acoustic backscattering from the deep seafloor with Seabeam," *J. Acoust. Soc. Am.* **79**, 316-331 (1986).
5. X. Lurton, *An Introduction to Underwater Acoustics: Principle and Applications* (PRAXIS, Chichester, 2002), Chap. 8, pp. 247-292.

6. D. R. Jackson, D. P. Winebrenner, and A. Ishimaru, "Application of the composite roughness model to high-frequency bottom backscattering," *J. Acoust. Soc. Am.* **79**, 1410-1422 (1986).
7. C. de Moustier and D. Alexandrou, "Angular dependence of 12-kHz seafloor acoustic backscatter," *J. Acoust. Soc. Am.* **90**(1), 522-531 (1991).
8. Z. H. Michalopoulos, D. Alexandrou, and C. de Moustier, "Application of neural and statistical classifiers to the problem of seafloor characterization," *IEEE J. Ocean Eng.* **20**, 190-197 (1995).
9. B. Chakraborty, E. Lourenco, V. Kodagali, and J. Baracho, "Application of artificial neural networks to segmentation and classification of topographic profiles of ridge-flank seafloor," *Curr. Sci.* **85**, 306-312 (2003).
10. W. A. Fernandes and B. Chakraborty, "Multi-beam backscatter image data processing techniques employed to EM 1002 system," in *Proceedings of the International Symposium on Ocean Electronics*, Kochi, India (2009), pp. 93-99.
11. K. Haris, B. Chakraborty, C. De, R. G. Prabhudesai, and W. A. Fernandes, "Model-based seafloor characterization employing multi-beam angular backscatter data - A comparative study with dual-frequency single beam," *J. Acoust. Soc. Am.* **130**(6), 3623-3632 (2011).
12. C. De and B. Chakraborty, "Model based acoustic remote sensing of seafloor characteristics," *IEEE Trans. Geosci. Rem. Sens.* **49**(10), 3868-3877 (2011).
13. C. De and B. Chakraborty, "Estimation of mean grain size of seafloor sediments using neural network," *Mar. Geophys. Res.* **33**, 45-53 (2012).
14. C. De and B. Chakraborty, "Acoustic characterization of seafloor sediment employing a hybrid method of neural network architecture and fuzzy algorithm," *IEEE Geosci. Rem. Sens. Lett.* **6**(4), 743-747 (2009).
15. A. Malinverno, "Segmentation of topographic profiles of the sea floor based on a Self-affine model," *IEEE J. Ocean Eng.* **14**, 348-359 (1989).
16. B. Chakraborty, V. Kodagali, and J. Baracho, "Seafloor classification using multibeam echo sounder angular backscatter data: A real time approach employing hybrid neural network architecture," *IEEE J. Oceanic Eng.* **28**, 121-128 (2003).
17. B. Chakraborty, R. Kaustubha, A. Hegde, and A. Pereira, "Acoustic seafloor sediment classification using self-organizing feature maps," *IEEE Trans. Geosci. Rem. Sens.* **39**, 2722-2725 (2001).
18. B. Chakraborty, V. Mahale, C. de Sousa, and P. Das, "Seafloor classification using echo-waveforms: a method employing hybrid neural network architecture," *IEEE Geosci. Rem. Sens. Lett.* **1**, 196-200 (2004).
19. S. Dandapath, B. Chakraborty, S. M. Karisiddaiah, A. Menezes, G. Ranade, W. Fernandes, D. K. Naik, and K. N. Prudhvi Raju, "Morphology of pockmarks along the western continental margin of India: employing multibeam bathymetry and backscatter data," *Mar. Petrol. Geol.* **27**, 2107-2117 (2010).
20. S. Dandapath, B. Chakraborty, N. Maslov, S. M. Karisiddaiah, D. Ghosh, W. Fernandes, and A. Menezes, "Characterization of seafloor pockmark seepage of hydrocarbons employing fractal: A case study from the western continental margin of India," *Mar. Petrol. Geol.* **29**, 115-128 (2012).
21. D. D. Sternlicht and C. P. de Moustier, "Time dependent seafloor acoustic backscatter (10-100 kHz)," *J. Acoust. Soc. Am.* **114**, 2709-2725 (2003).
22. D. D. Sternlicht and C. P. de Moustier, "Remote sensing of sediment characteristics by optimized echo-envelope matching," *J. Acoust. Soc. Am.* **114**, 2727-2743 (2003).
23. D. R. Jackson and K. B. Briggs, "High-frequency bottom backscattering: Roughness vs. sediment volume scattering," *J. Acoust. Soc. Am.* **92**, 962-977 (1992).
24. R. A. Stewart and N. P. Chotiros, "Estimation of sediment volume scattering cross section and absorption loss coefficient," *J. Acoust. Soc. Am.* **91**, 3242-3247 (1992).